

Section D – Engineering & ICT

Fault Analysis and Protection of DC MicroGrids

A Imantha¹, P Binduhewa¹, J Ekanayake^{1*}, K Liyanage¹

University of Peradeniya

*Corresponding Author: jbe@ee.pdn.ac.lk

Abstract—More efficient installation techniques, lower costs of capital, and improved supply chains has brought down the cost of solar PV. This has triggered direct use of PV output in a dc MicroGrid. A MicroGrid is a small independently controlled electric network powered by local distributed energy sources that can be operated in the grid-connected and islanded modes. A dc MicroGrid allows to connect solar PV without any conversion stages and also allows to connect many loads that are predominantly dc to the grid without ac to dc conversion stages. Even though dc MicroGrids are considered for commercial and large building environments, their fault performance are yet to be investigated. In this paper, the fault current for a dc side fault is considered and protection measures are highlighted.

Keywords—dc micro grid, fault analysis, protection

I. INTRODUCTION

In most of the renewable energy based power generation systems, a final dc to ac power conversion stage is used to connect the source to the ac grid. For example, in solar PV applications a dc to ac converter is used at the final stage. In wind power applications ac output of the wind generator is first converted to dc and then again converted back to ac to connect to the ac grids. Instead, if the grid is dc then one converter stage can be removed in such applications. Further, entertainment equipment, compact fluorescent lamps, LED lamps and emerging technologies, such as variable frequency drives (VFDs) that use dc are growing. Currently, these loads are connected to the ac network through ac/dc conversion stages. The above approach, connecting PV and loads through conversion stages to the distribution networks, reduces efficiency, increases initial costs, as well as total cost of ownership due to power losses at each conversion point.

A dc MicroGrid enables a common platform to connect most of renewable energy sources and dc loads in an efficient manner. In a dc MicroGrid there are sources, energy storages and loads connected to dc link with or without converters depending on their voltage level.

II. DC MICROGRID TOPOLOGIES

A. Single bus topology

Single bus topology is the widely used architecture of the dc MicroGrids. As give in Fig. 1 in this arrangement there is only a single dc link. All the sources are connected to the dc link through power electronics converters or directly. In this arrangement dc link voltage will be maintained by either using utility interfacing ac/dc converter or a battery stack. This

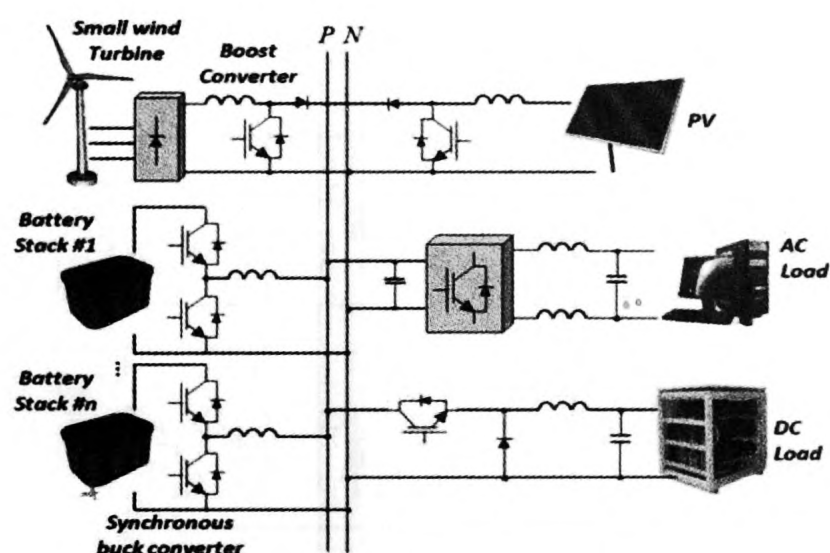


Fig. 1 Single bus topology [1]

topology is the most common among telecommunication applications operating at 48V.

However as there is only a single dc bus to which all the loads and sources are connected, the reliability of this system is low. To overcome this issue several remedies were proposed. Among them bipolar single regulated bus structure shows a higher increment of reliability [2]. As shown in Fig.2 this configuration has three lines on distribution end which allows load interfacing converters to select voltage levels between +340V, +170V and -170V. In case of single pole failure, there

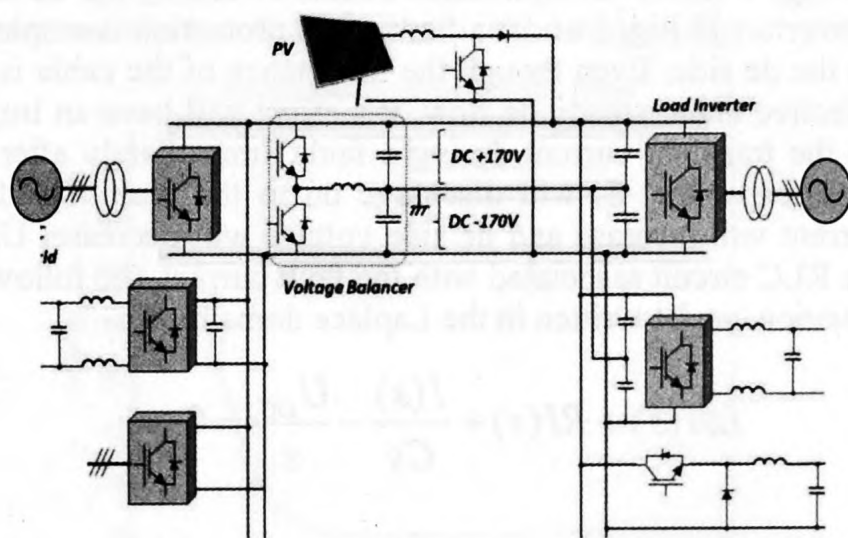


Fig. 2 Bipolar single regulated bus structure [2]

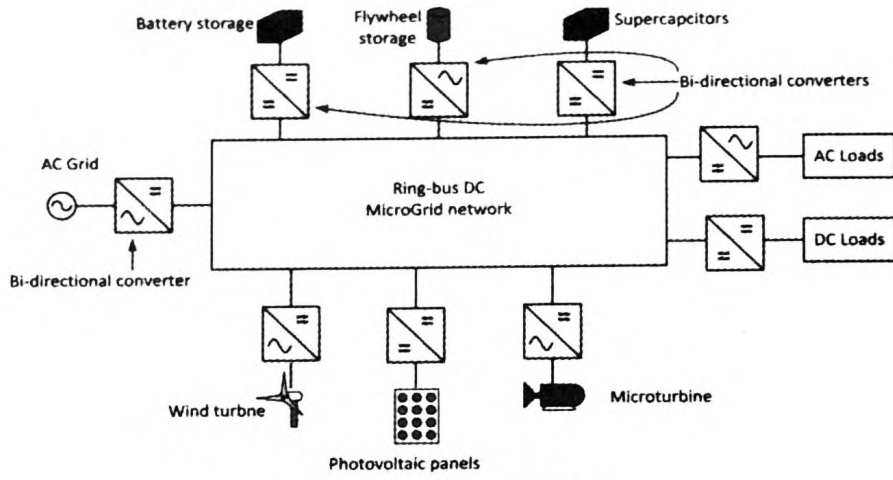


Fig. 3 Ring bus topology

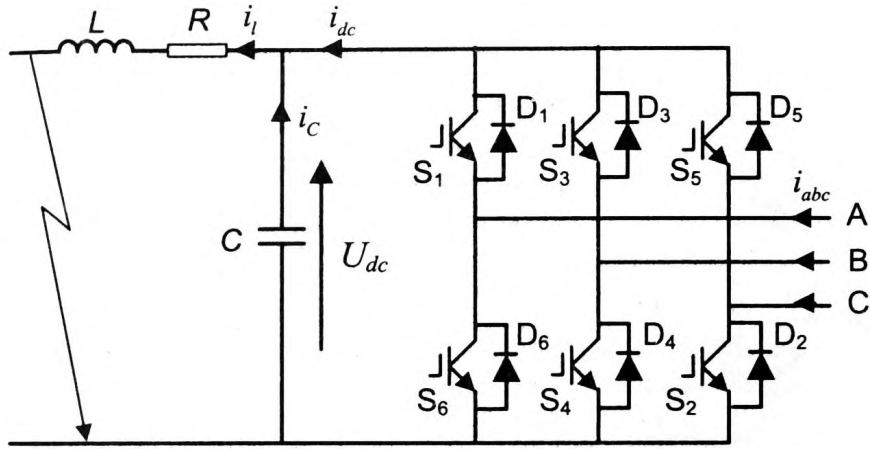


Fig. 4 An equivalent circuit of each VSC under dc side fault

is still possibility to supply power using other two lines. However since there are two power poles, it requires an additional voltage balancer mechanism to maintain the voltage between each pole and common wire.

B. Ring bus topology

Fig. 3 shows a ring bus configuration [3]. Because of ring configuration each node can be supplied using two directions and there is a bi-directional power flow within the network. Thus it improves redundancy and reliability of the power flow within the MicroGrid.

III. DC SIDE FAULT

Fig. 4 shows an equivalent circuit of one of the ac to dc converters in Fig. 3 under a fault; if no protection is employed on the dc side. Even though the inductance of the cable is not effective under steady dc flow, it's effect will have an impact on the transient current during a fault. Immediately after the fault, capacitor, C, will discharge on to the fault. The fault current will increase and dc side voltage will decrease. Using the RLC circuit associated with the fault current, the following equation can be written in the Laplace domain:

$$LsI(s) + RI(s) + \frac{I(s)}{Cs} - \frac{U_{DC}}{s} = 0$$

$$I(s) = \frac{CU_{DC}}{LCs^2 + RCs + 1} = \frac{U_{DC}}{L} \left[\frac{1}{s^2 + \frac{R}{L}s + \frac{1}{LC}} \right] \quad (1)$$

The denominator of Equation (1) is written in the following form:

$$s^2 + \frac{R}{L}s + \frac{1}{LC} = (s + \alpha)(s + \beta)$$

where

$$\alpha = \frac{1}{2} \left[\frac{R}{L} - \sqrt{\frac{R^2}{L^2} - \frac{4}{LC}} \right]$$

$$\beta = \frac{1}{2} \left[\frac{R}{L} + \sqrt{\frac{R^2}{L^2} - \frac{4}{LC}} \right]$$

Using partial fraction of Equation (1):

$$I(s) = \frac{U_{DC}}{L} \left[\frac{A}{(s + \alpha)} + \frac{B}{(s + \beta)} \right] \quad (2)$$

where

$$A = -B = \frac{1}{(\beta - \alpha)} = \frac{1}{\sqrt{\frac{R^2}{L^2} - \frac{4}{LC}}}$$

Taking inverse Laplace transform of Equation (2):

$$i(t) = \frac{U_{dc}}{\sqrt{R^2 - 4L/C}} \left[e^{-\alpha t} - e^{-\beta t} \right] \quad (3)$$

The shape of $i(t)$ depends on α and β .

When $R^2 > \frac{4L}{C}$, α and β are real and therefore $i(t)$ changes exponentially.

When $R^2 < \frac{4L}{C}$, α and β are complex. Then

$$i(t) = \frac{2U_{dc}}{\sqrt{4L/C - R^2}} e^{-\frac{R}{2L}t} \sin \left[\left(\frac{1}{2} \sqrt{\frac{4}{LC} - \frac{R^2}{L^2}} \right) t \right]$$

In Laplace domain, the capacitor voltage is given by

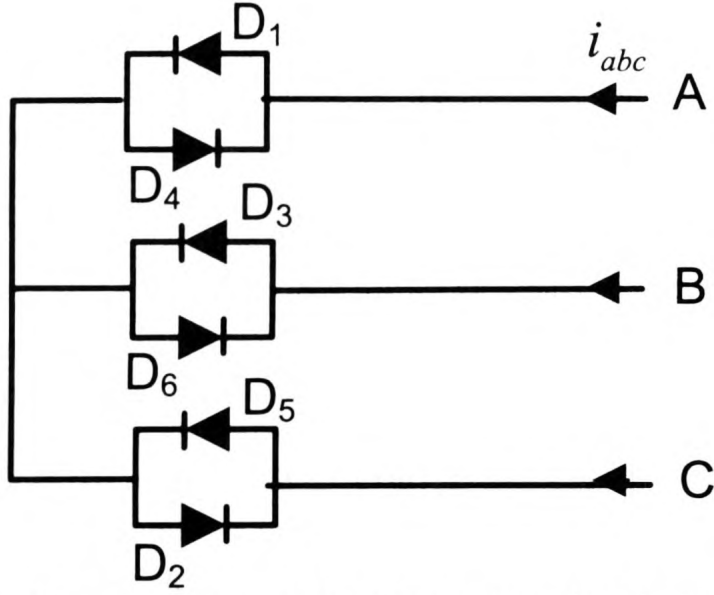


Fig. 5 An equivalent circuit when the capacitor is fully discharged

$$U_{dc}(s) = \frac{AU_{DC}}{L} \left[\frac{1}{(s+\alpha)} - \frac{1}{(s+\beta)} \right] [R+Ls]$$

$$= \frac{U_{DC}}{L} \left[\frac{AR-AL\alpha}{(s+\alpha)} - \frac{AR-AL\beta}{(s+\beta)} \right]$$

Taking inverse Laplace Transform:

$$U_{dc}(t) = \frac{AU_{DC}}{L} \left[(R-L\alpha)e^{-\alpha t} - (R-L\beta)e^{-\beta t} \right] \quad (4)$$

From Equation (4), it can be seen that when $t=0$, $U_{dc}(t) = U_{DC}$

As dc voltage drops, freewheeling diodes, D₁ to D₆ get forward biased. Therefore, on top of the capacitor discharge current a small current passes from ac side to dc side through freewheeling diodes. When the capacitor is fully discharged, the capacitor acts as a short circuit to ac side through freewheeling diodes as shown in Fig 5. This result in a large current, similar to a three-phase fault current, flows on the ac side. The dc fault current continue to fall.

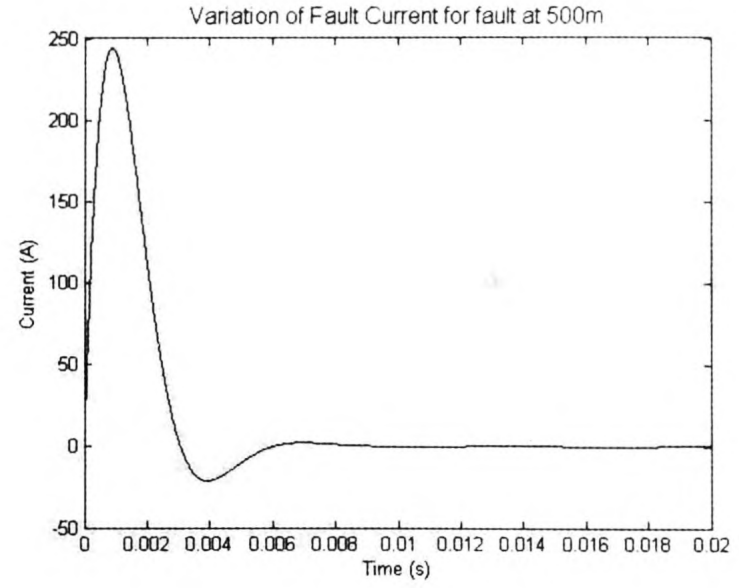
IV. CASE STUDY

A ring MicroGrid operating at 380 V uses a dc capacitor of 1000 uF and a Single core PVC insulated cable of 10 mm². The cable has the following parameters:

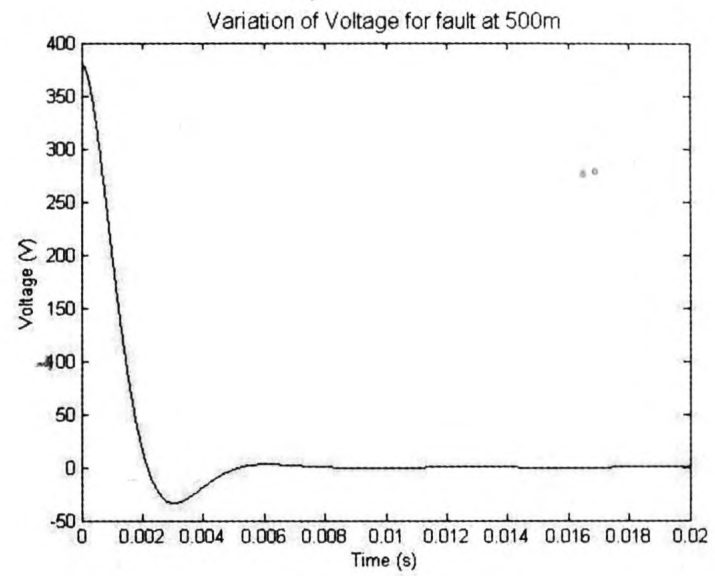
Resistance per km = 1.88Ω

Inductance per km = 1.18mH

First fault occur after 500m from the ac to dc converter. The waveforms of current and voltage just after the fault is shown in Fig. 6



a) Fault Current

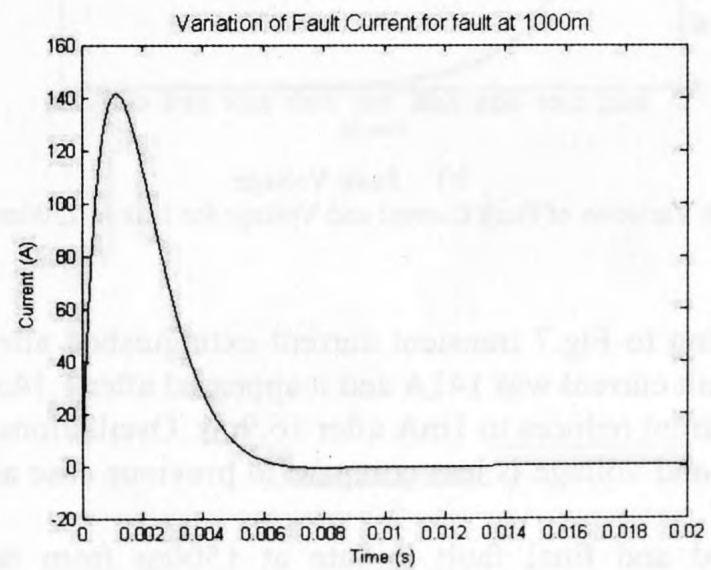


b) Fault Voltage

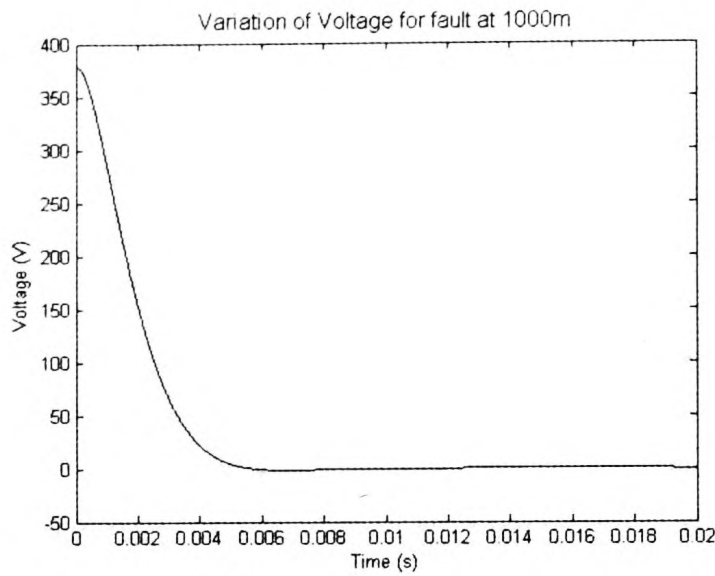
Fig. 6. Variation of Fault Current and Voltage for fault at 500m

For 500m effective resistance and inductance for fault current path are 0.89Ω and 0.59mH respectively. As shown in Fig 6 the fault transient lasted for 7ms duration. It was observed that the peak fault current is 244A and it appears after 0.89ms from occurrence of the fault. After 15ms fault current reduced to 1mA.

In second test case the fault occurs after 1000m from the ac to dc converter. Thus the resistance of 1.88Ω and inductance of 1.18mH applied for the fault current path. The voltage and current waveforms of this test case is showing in Fig.7.

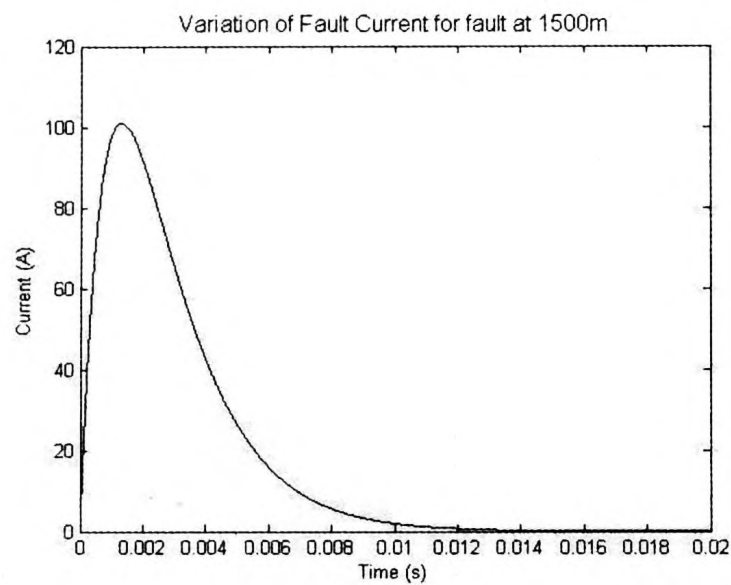


a) Fault current

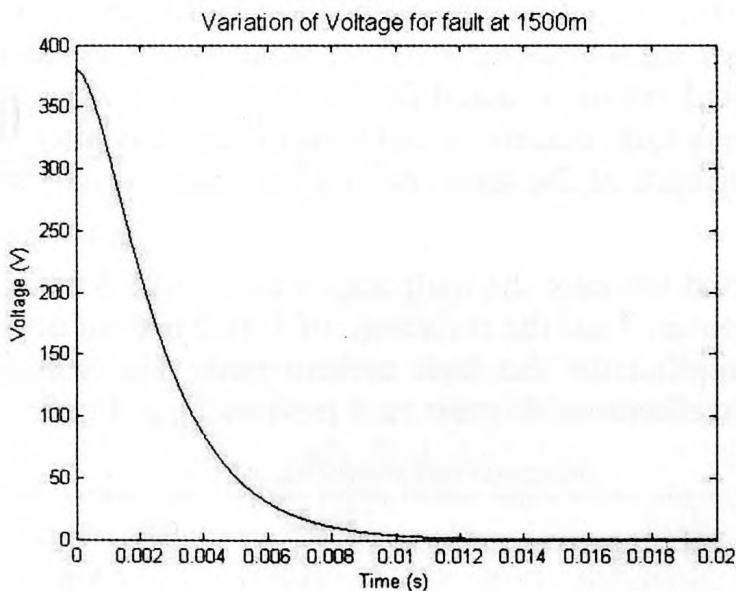


b) Fault voltage

Fig. 7. Variation of Fault Current and Voltage for fault at 1000m



a) Fault Current



b) Fault Voltage

Fig. 8 Variation of Fault Current and Voltage for fault at 1500m

According to Fig.7 transient current extinguished after 10ms. Peak fault current was 141A and it appeared after 1.14ms. Also fault current reduces to 1mA after 16.9ms. Oscillations of fault current and voltage is less compare to previous case as shown in Fig 7.

Third and final fault initiate at 1500m from the main converter and corresponding waveforms of current and voltage

given in Fig 8. Fault current flow through a resistances of 2.88Ω and inductance of 1.77mH in series.

As shown in Fig.8 current and voltage transients extinguished after 12ms. Since this fault occurs at the furthest end from the ac to dc converter it has a less peak fault current compare to previous two cases. It recorded as 101A and appeared after 1.3ms from the fault occurrence.

By looking at the results it can see that when the distance is increasing the peak of the fault current is reducing. Though the peak fault current reduced duration of the existence of fault current is increasing with the distance.

Also in first two cases α and β are complex values. Thus it causes a small ripple in fault current and voltages (this is not visible in Fig.6 and Fig 7). However, in third case where α and β are real values there is no such ripples in current and voltage waveforms.

V. PROTECTION

DC network protection is an area which is still emerging in the nature. Fuses and Miniature Circuit Breakers (MCB) are the commonly used equipment as protective devices.

Fuse is the simplest protective device widely used in industrial dc power applications. Most of the time it has been suggested that fuses will perform better in systems having low inductance. Because of low inductance this kind of systems can have a higher rate of change of current which causes to melt down the contacting link in fuses rapidly during a fault condition.

On the other hand MCBs are used for over current and short circuit protection. In general these protection functionalities will be acquired through thermal-magnetic tripping mechanism. [4]

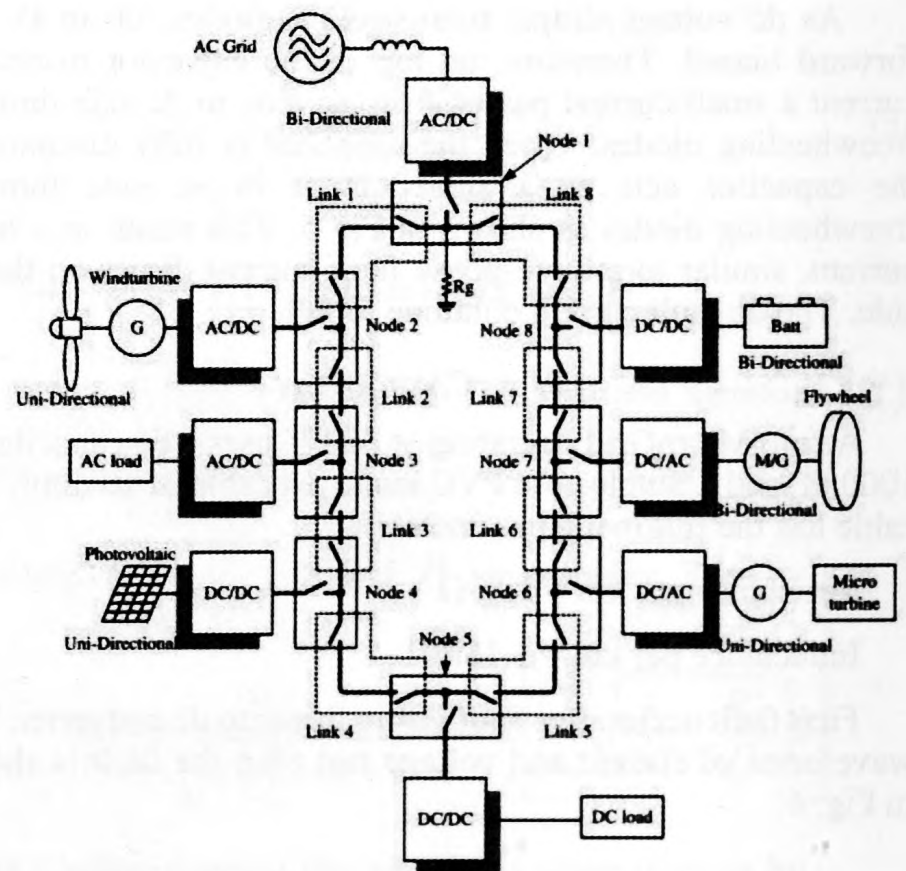


Fig.9. Protection applied to a ring dc MicroGrid [3]

As shown in Fig. 6 to Fig 8 the peak fault current has a magnitude above 100A and it occurs around 1ms.

For close faults, entire fault transient will last less than 2ms if the fault current allows to extinguish naturally. If dc side protective devices operate before this transient, then ac side current will not be high enough to operate the fuses that are being employed to protect the inverter. However if capacitor is fully discharged then ac side current increases drastically thus operating the ac side fuses.

Fig.9 shows the typical protection scheme applied to a ring configuration. In this configuration each node and link between two neighboring nodes are connected using fuses or MCBs. In order to isolate the dc side fault and operates the ring without the faulty section, the dc side protective devices should be operated within less than 1ms duration. For an MCB this operating time is significant. The required force to operate the breaking mechanism of circuit breaker may not be generated within such short time period in some instances. Similarly the fuse may not be properly disconnected by melting the conducting element. Thus a careful design criteria may need to follow in order to implement a proper protection in dc distribution network.

To overcome these challenges semiconductor based CBs can be used in the system. These devices equipped with faster switching actions compare to common CBs. However since these devices equipped with semiconductor elements there will be an additional energy loss which may affect to the overall efficiency of the network.

VI. CONCLUSIONS

A fault current contribution for a dc side fault is investigated. The fault current contribution was analytically obtained and a case study was used to demonstrate the fault transient. In order to operate a dc ring satisfactorily the fault should be cleared from the dc side. As fault current diminishes around 2 ms for close faults, a fast acting MCB should be used.

ACKNOWLEDGMENT

Authors wish to acknowledge the financial support provided by the National Research Council under the research grant No: NRC 14 -15 and Sustainable Energy Authority.

REFERENCES

- [1] T. Dragičević, X. Lu, J. C. Vasquez, and J. M. Guerrero, "DC Microgrids—Part II: A Review of Power Architectures, Applications, and Standardization Issues", *IEEE Transactions On Power Electronics*, Vol. 31, No. 5, May 2016 pp. 3528 – 3549
- [2] H. Kakigano, Y. Miura, and T. Ise, "Low-voltage bipolar-type DC micro-grid for super high quality distribution," *IEEE Transaction on Power Electronics*, vol. 25, No. 12, Dec. 2010, pp. 3066–3075.
- [3] J.D. Park, J. Candelaria, L. Ma, and K. Dunn, "DC ring-bus microgrid fault protection and identification of fault location," *IEEE Transaction on Power Delivery*, vol. 28, no. 4, pp. 2574–2584, Oct. 2013.
- [4] R. M. Cuzner and G. Venkataramanan, "The status of DC microgrid protection," in *Proceedings IEEE Industrial Applications Society Annual Meeting*, 2008, pp. 1–8.